INDMF Based Regularity Calculation Method and Its Application in the Recognition of Typical Loess Landforms

Sheng Jiang [1], Xiaoli Huang [2,*] and Ling Jiang [2]

[1] School of Mechatronics and Information, Wuxi Vocational Institute of Arts and Technology, Yixing 214206, China; jiangsheng@wxgyxy.edu.cn

[2] School of Geographical Information and Tourism, Chuzhou University, Chuzhou 239000, China; ling.jiang@chzu.edu.cn

[*] Correspondence: huangxl@chzu.edu.cn; Tel.: +86-156-5197-6189

Abstract: The topographical morphology of the loess landform on the Loess Plateau exhibits remarkable textural features at different spatial scales. However, existing topographic texture analysis studies on the Loess Plateau are usually dominated by statistical characteristics and are missing structural characteristics. At the same time, there is a lack of regularity calculation methods for DEM digital terrain analysis. Taking the Loess Plateau as the study area, a regularity calculation method based on the improved normalized distance matching function (INDMF) is proposed and applied to the classification of a loess landform. The regularity calculation method used in this study (INDMF regularity) mainly includes two key steps. Step 1 calculates the INDMF sequence value and the peak and valley values for the terrain data. Step 2 calculates the significant peak and valley, constructs the significant peak and valley sequences, and then obtains the regularity using the normalised ratio value. The experimental results show that the proposed method has good anti-interference ability and can effectively extract the regularity of the main landform unit. Compared with previous methods, adding structural features (i.e., INDMF regularity) can effectively distinguish loess hill and loess ridge in the hilly and gully region. For the loess hill and loess ridge, the recognition rates of the proposed method are 84.62% and 92.86%, respectively. Combined with the existing topographic characteristics, the proposed INDMF regularity is a topographic structure feature extraction method that can effectively discriminate between loess hill and loess ridge areas on the Loess Plateau.

Keywords: DEM; loess hilly and gully region; INDMF regularity; terrain texture; landform recognition; Loess Plateau

1. Introduction

China's Loess Plateau has experienced more than two million years of loess transportation and accumulation. Under various factors, it has developed into the geomorphic characteristics of "thousands of gullies" based on the ancient landform of rock strata. Many scholars have studied the landform of the Loess Plateau from different perspectives: many research achievements have been made in the causes of the Loess Plateau [1–3], the mode of loess erosion [4,5], the development of loess landform [6–8]. These results clarify the significance of the Loess Plateau in the material and energy cycle and ecological environment protection in China and even the world. In addition, with the development of sensor technology and remote sensing technology, DEM data is becoming one of the key data for the study of China's Loess Plateau [9–13].

The topography of the Loess Plateau has significant self-similarity [14], which makes it feasible to study the terrain quantification, recognition and classification of the Loess Plateau by using texture features [15,16]. Figure 1 is a visualisation of the DEM (Digital Elevation Model) for typical landforms of the Loess Plateau. Figure 1a presents the early stage of loess tableland. Figure 1b shows the late stage of loess tableland. Figure 1c is the loess ridge area. Figure 1d is the loess hill area. These four samples are distributed

sequentially from south to north, the gully erosion gradually intensifies, and the texture primitives visually change from coarse to fine. At the same time, the gullies themselves and their spatial distribution have significant self-similarity. The research on the self-similarity topographic characteristics and spatial distribution law of the Loess Plateau has important theoretical significance and application prospects for clarifying the spatial pattern of soil erosion on the Loess Plateau [4], guiding the protection of soil and water loss on the Loess Plateau [17,18], optimizing land use evaluation [19].
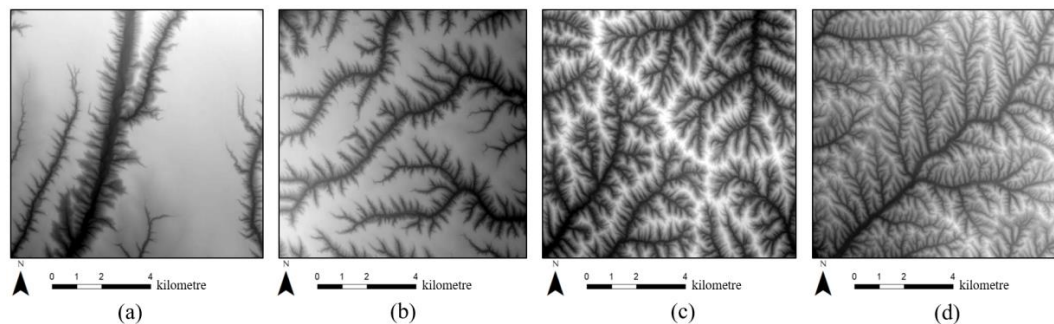
Figure 1. DEM visualisation of typical landform of Loess Plateau. (**a**) the early stage of loess tableland; (**b**) the late stage of loess tableland; (**c**) loess ridge area; (**d**) loess hill area.

The self-similarity of the Loess Plateau can be calculated and quantified by texture analysis. With the development of aerial sensors, data acquisition technology for high-resolution remote sensing images and digital elevation models has been widely used. Texture analysis has been an important means of geomorphic mapping and terrain classification in the field of geoscience [20,21]. Many research works have applied textural features to the digital topography analysis of the Loess Plateau. In 2011, Tao [22] elaborated on the concept of topographic texture. In his loess topography analysis, the author performed scale analysis and quantitative feature comparison by using the moment invariant, GLCM (Gray-level Co-occurrence Matrix) texture operator and three-dimensional porosity methods which verify the effectiveness of texture features for loess landform recognition and classification. On the basis of a DEM and remote sensing image data, Liu et al. [23] analysed the differences in the texture features of the Loess Plateau. The authors selected eight different geomorphic sample areas to compare and analyse the effectiveness, stability and intergroup differences of topographic features. His experimental results show significant differences in texture features between the DEM and the remote sensing images. The DEM can more directly describe the feature changes caused by topographic fluctuations, and remote sensing images are greatly affected by the loess surface cover. In recent years, with the continuous progress of soil and water conservation in the Loess Plateau, DEM has gained significant advantages in the topographic analysis of the Loess Plateau. In addition, the derived factors of the DEM, such as the second-order texture features of slope and illumination simulation, also have good intergroup discrimination. Then, aiming at the stability of the texture features of topographic relief in the loess landform, Huang et al. [24] and Li et al. [25] analysed the degree of texture change through the GLCM and RILBP (Rotation-Invariant Local Binary Pattern) methods, respectively. Both methods clearly show that the resolution of the DEM has a significant impact on texture recognition, and different resolutions lead to different recognition efficiencies and result accuracies. Huang adjusted the texture parameters of the GLCM operator, compared them item by item and found that four parameters in multiple features have a good recognition rate. Li et al. [25] also considered the significant impact of scale, and different loess landforms have different stability scales. Ding et al. [26] used 48 random loess areas, and the terrain texture measure was significantly correlated with the gully density, slope and other terrain factors, indicating that the terrain texture measure based on the stability analysis unit can reflect the basic characteristics of the topographic morphology.

From the above literature, we can know that texture features are gradually applied in the topographic analysis of the Loess Plateau from theoretical research. Although the amount of relevant literature is limited, feasible conclusions have been given on the applicability of texture features in the topographic analysis of the Loess Plateau. However, the current research is mostly based on the statistical method, which is based on the probability density distribution between pixels. There are few cases of texture analysis using structural features.

The above method is mainly used in theoretical research on the texture features of the loess landform. In recent years, texture features have been applied to practical classification and recognition. Zhao et al. [27] constructed a combination of topographic characteristics (e.g., mean slope and elevation range) and textural characteristics (e.g., slope contrast and elevation variance) on the basis of the SRTM (Shuttle Radar Topography Mission) DEM data, using small watersheds at a regional scale. The authors found that the highest accuracies were obtained in the Loess station and the loess mountain among the seven typical loess landforms. At the same time, relatively low recognition accuracies were obtained for loess hills, ridges and slopes, although the overall recognition accuracies are better than those of the features without texture. Li et al. [28] researched the slippery slope identification method based on the combination of DEM and remote sensing imaging data. On the basis of the comprehensive analysis of six features, such as roughness, cutting degree and undulation, the neural network is used for nonlinear combination and supplemented with the NDVI (Normalized Difference Vegetation Index) for identification. The results show that the accuracy recognition rate for landslides is 71.03%, indicating that the landslide range can be well-identified. Using the nine statistical features [9] obtained by the GLCM method, Ding took Zhifang's small watershed as the measured area to improve the recognition accuracy of the positive and negative terrains in the loess's small watershed, and the recognition accuracy improved by almost 6%, thereby optimising the accuracy of the positive and negative terrain mapping in small watersheds. In recent years, object-oriented methods have been used in loess landform recognition and classification, and texture features are classified as a very important basic feature [29]. Texture features can improve the accuracy of classification and recognition [15,30–32].

The above literature review indicates that the texture feature based on DEM has been applied in the Loess Plateau and made achievements in topography recognition and classification. However, the current texture features are mainly statistical. These features mainly use the GLCM method and the probability density distribution between pixels for the pattern recognition of the topography [33,34]. In the Loess hilly and gully area, loess hill and loess ridge are difficult to distinguish based on the textural characteristics obtained by the GLCM, according to the literature and previous experiments [14,22,23]. Therefore, the use of the texture structure characteristics of loess to improve the accuracy of recognition and classification is an important part of texture methods in topographic analysis [20,35]. In addition, the combination of texture and structural features can form a uniform framework for texture methods and expand new methods for digital terrain analysis [36].

From the above literature analysis, we can know that the geomorphic units in the hilly and gully areas of the Loess Plateau have strong structural self-similarity, but structural texture features are rarely used in analysis and processing. Haralick [33] divided textures into two types: tone dominated, and structure dominated. Among them, structure-dominated texture is also called approximate regular texture, which emphasizes the spatial relationship between texture primitives. Regularity, or periodicity, is an important index for the description and classification of approximate regular texture features [37]. At present, one of the main ideas to calculate the regularity is to extract features first and then perform periodic operations. The feature extraction methods include autocorrelation function [38,39], Fourier spectrum feature [40,41], vertical and horizontal section line [42] and grey level co-occurrence matrix (GLCM) feature [43], and then several methods are used to calculate the period and regularity based on the extracted features. However, these

methods still have the following shortcomings: (1) parameter setting. For example, the automatic performance of the autocorrelation method is limited by parameter setting, which is difficult to set automatically. (2) Noise interference problem: noise interferes with peak extraction, such as extracting texture curve features in remote sensing images by vertical and horizontal section line method, which is often interfered with by noise and secondary texture primitives, so as to extract falser peak and valley values. In order to reduce the adverse effects of the above problems, the distance matching function (DMF) was proposed by Oh, et al. [44]. Subsequently, Asha, et al. [45] proposed the sum-up distance matching function (SDMF). The experimental results in Asha's paper show that the SDMF method can extract the period of the texture image quickly, with good accuracy and stability. The principle of the DMF and SDMF method is that the grey periodic change on the texture image is used as a key texture index for texture classification and recognition [42,46,47]. Therefore, the SDMF has a practical application value. For automatic period extraction based on the SDMF, the distance of the first peak is usually used as the period of the entire texture image [48]. However, using only the first peak as the period, the anti-interference ability against noise and geometric distortion is relatively weak. To improve the reliability of extracting the structural texture period, Jiang et al. proposed an improved normalised DMF (INDMF) method [49].

Taking INDMF as the basic model, this paper will build a terrain regularity calculation method based on DEM data. This method can effectively reduce various interference factors in the terrain and extract the regularity of main landform units. In addition, the regularity is applied to the classification of loess landform, so as to improve the recognition accuracy of hilly areas of the Loess Plateau. Finally, the application scope of the proposed regularity is also discussed in this paper. The authors also expect that this method can expand and deepen the application scope of DEM digital terrain quantification research.

2. Materials and Methods

2.1. Study Area and Sample Data

The study and sample areas in this study are shown in Figure 2. The sample area is located northwest of the neotectonic movement zoning line, mainly because this area includes typical loess landforms, such as loess tableland, residual tableland, loess hill, loess ridge and mountain areas [50]. This area also includes some areas with low erosion, such as the sand-covered loess and rocky mountainous areas, which meet the research requirements in terms of topographic typicality and comprehensiveness.
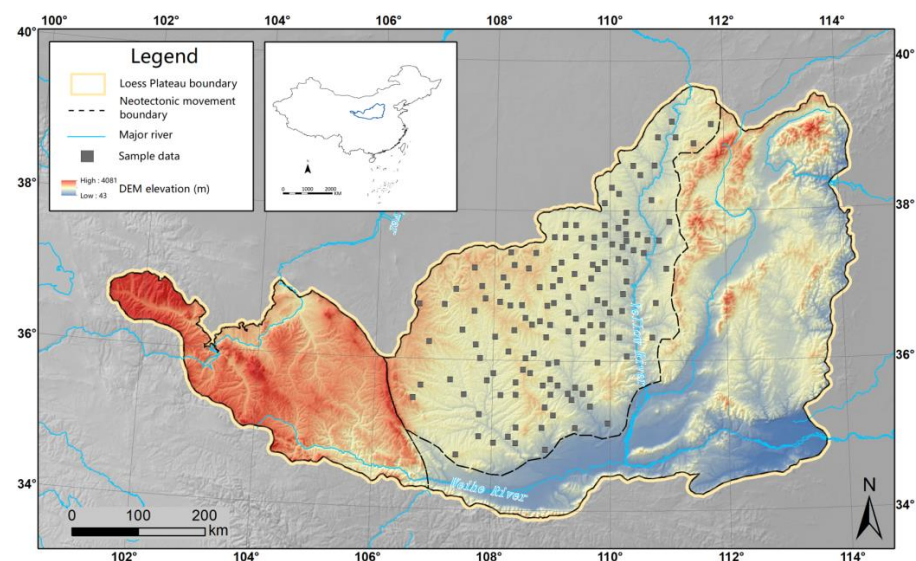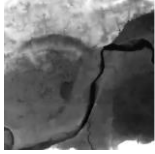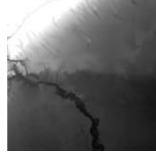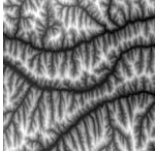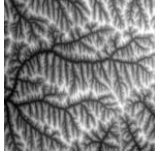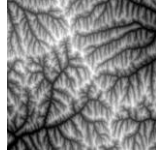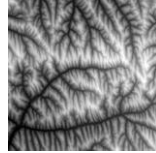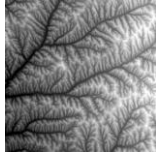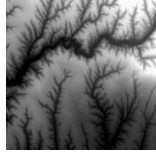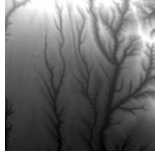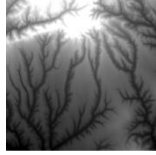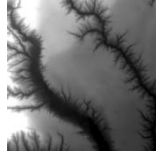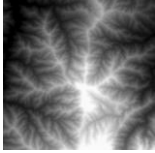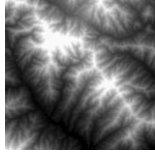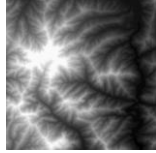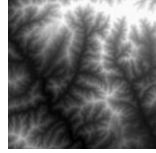

Figure 2. Study area and sample data.

A total of 138 sample areas are used (see Figure 2 for details). Of these sample areas, 28 are used as training data, 77 as test data and 33 as confusion data. The confusion data are mainly transitional areas or areas with atypical geomorphic types.

In this paper, the typical landforms of loess are classified into seven categories: the loess plain, loess ridge, loess hill, loess long ridge residual tableland, loess residual tableland, loess tableland and loess mountain area. For each category, four similar geomorphic types are selected, 28 samples are used as training samples, and the remaining 77 data are used as test data. The visual schematic of the training samples is shown in Table 1. For samples of the different sample areas, the selection is as representative as possible, significantly reflecting the geomorphic characteristics of the sample areas and avoiding the transition areas between different sample areas as far as possible. For the unavoidable transition areas, the selection of a sample with a dominant appearance is attempted. For similar samples, the selection principle is consistent. The sample size is divided into 512 × 512 pixels by referring to the existing research results [22,51].

Table 1. Training samples of typical landforms.

Landform Type	Sample 1	Sample 2	Sample 3	Sample 4
loess plain				
loess ridge				
loess hill				
loess long ridge residual tableland				
loess tableland				
loess residual tableland				
loess mountain				

The selection of sample data is based on the following principle. For a Loess Plateau study sample area facing a small watershed, the most important principle is that sample selection needs typicality. Typicality is the need to select representative areas of commonalities in terms of individuality and, thus, in terms of typicality. For the region-oriented Loess Plateau study sample, the essential principles are diversity and integrity. The sample area's diversity and completeness will directly determine its reliability for the entire study.

The ground sampling distance of the DEM data used in this study is 25 m/pixel. The DEM data used in this paper was produced by Shaanxi Surveying and Mapping Bureau through aerial photogrammetry combined with postproduction. At the same time, aerial images and ground control points were also collected by the Shaanxi Surveying and Mapping Bureau. Gaussian Kluger projection was adopted, using the 1980 national geodesic coordinate system and the 1985 national elevation datum. The production process follows the data production process in the technical regulations for the production of a digital elevation model. In this process, the DEM generation method is used to construct the tin from the digital topographic map contour. Then, it is interpolated into a regular grid DEM. According to the actual measurement, the data can meet the accuracy requirements of this study. The DEM data used in this paper is produced by the Shaanxi Bureau of Surveying and mapping. The original data of the DEM data is a contour topographic map. Therefore, after digitizing the contour lines, engineers use ArcGIS software to generate TIN, and then interpolate it into regular grid DEM.

2.2. Methods

2.2.1. INDMF Regularity Calculation

The distance matching function (DMF) was proposed by Oh et al. in 1999 [44]. To improve the reliability of extracting the structural texture period, Jiang et al. proposed an improved normalised DMF (INDMF) method [49]. This method uses the step length with the longest lifetime in the period, i.e., the mode, as the period index. For image $f(x,y)$ of M rows and N columns, the INDMF in the row and column directions are expressed as:

$$\text{INDMF}_r(d) = \frac{1}{(M-d) \times N} \sum_{j=1}^{N} \sum_{i=1}^{M-d} |f(i,j) - f(i+d,j)| \tag{1}$$

$$\text{INDMF}_c(d) = \frac{1}{(N-d) \times M} \sum_{j=1}^{N-d} \sum_{i=1}^{M} |f(i,j) - f(i,j+d)| \tag{2}$$

where $\text{INDMF}_r(d)$ represents the INDMF value with pixel distance d, and r represents the number of lines in the image, i.e., the horizontal direction. Similarly, c represents the number of columns in the image, i.e., the vertical direction. M and N, respectively, represent the length and width of the image, and I and j, respectively, represent the position of the row and column where the central pixel of the analysis window is located. In this paper, row direction and column direction are used for calculation. The regularity calculation of row and column directions is the most basic description of texture primitives. The outer rectangular range of rectangular texture primitives can be constructed through row period and column period.

The result of Jiang's experiment reveals that the INDMF formula has better anti-distortion and anti-noise ability than the original DMF and SDMF [49]. Given the complexity of the realistic geomorphic form, DEM data usually have much inevitable noise and geometric distortions. Therefore, the INDMF is suitable for the DEM data involved in this paper (the conclusion is obtained from the effectiveness experiment below). The INDMF can adjust the peaks and valleys of the periodic histogram to a unified scale, which is conducive to the periodic extraction of the gullies and valleys of the loess landform and the spatial positioning of the texture elements and optimise the stability of peak and valley extraction.

On the basis of the INDMF, this paper proposes the calculation method of the INDMF regularity. In regular or approximately regular texture images, period refers to the step

value of the repeated occurrence of texture primitives. Theoretically, the average step value of the directed sequence between peaks obtained by the INDMF should be equal or approximately equal to an integer multiple of the average distance between the texture primitives. However, the gullies of the loess landform show an approximate regular or random texture. If the gullies show an approximate regular texture, the step value difference of the sequence between the peaks calculated by the INDMF is within a certain threshold range. Otherwise, no significant sequence of peak and valley values exists. The flow chart of the calculation method of regularity based on the INDMF proposed in this paper is shown in Figure 3.
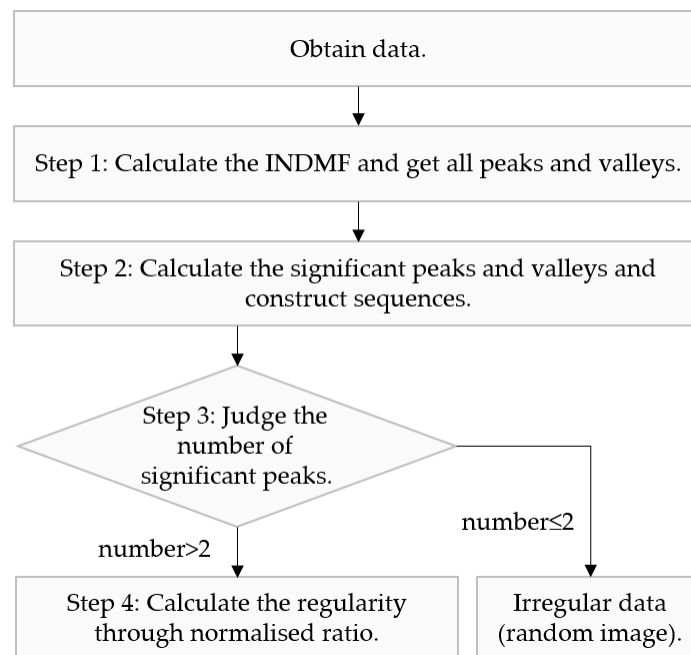
Figure 3. The flow chart of the INDMF regularity calculation method.

The calculation method of the INDMF regularity is described in detail as follows:

Step 1: Calculate the INDMF for the data and calculate all the peak and valley values of the INDMF sequence. $f(x)$ represents the INDMF, and its formula is shown in Formulas (1) and (2). It is a list of data sequences, which can be approximately regarded as a continuous function. On this basis, the data sequence is calculated. Let $f(x)$ have second derivative $f''(x)$ at point x_0, $f'(x) = 0$ and $f''(x) \neq 0$; when $f''(x) < 0$, function $f(x)$ at x_0 obtains the maximum value, i.e., the peak value; when $f''(x) > 0$, function $f(x)$ obtains the minimum value at x_0, i.e., the valley value.

Step 2: Calculate the significant peak and valley values according to the results of Step 1 and complete the construction of significant peak and valley sequences. Specifically, calculate the difference between the adjacent peak and valley values. When the difference is greater than or equal to a specific threshold, the peak is a significant peak and valley. After calculating many samples, this study confirms that it has good applicability when the specific threshold is set to $[\max(\text{INDMF}) - \min(\text{INDMF})]/20$.

Step 3: When the number of significant peaks and valleys is less than or equal to 2, the data is a random image, set the regularity to 0, and end the calculation. Otherwise, skip to Step 4.

Step 4: Calculate first period value d_1 and second period value d_2 on the basis of the sequence of significant peaks and then obtain the regularity through the normalised ratio. In the calculation of second periodic value d_2, derive the second-order derivative of the INDMF in the interval $[d_1 + 1, 3d_1 - 1]$ and obtain the maximum value. The above interval is selected to set the size range of second period d_2 as $[1, 2d_1]$, i.e., the minimum is 1 and the

maximum is twice the value of d_1. Its rationality has been confirmed in the literature [49]. The first and second periods are selected to calculate the regularity because the main period of the first two has optimal stability, so they can have the anti-interference ability caused by random factors. Regularity is denoted as R_n and expressed as Formula 3:

$$R_n = \frac{abs[d_1 - abs(d_2 - d_1)]}{d_1}, \ and \ d_1 \geq 1, \ (1 + d_1) < d_2 \leq (3d_1) \tag{3}$$

when first period value d_1 and second period value d_2 are equal, the normalised regularity is $R_n = 1$, and the regularity is the largest. When d_2 and d_1 exist and are not equal, the value range of R_n is (0, 1).

The first period value d_1 step of the above INDMF's significant peak can represent the size of the main texture primitive. The calculation of normalised regularity can be applied to the row and column directions of the INDMF and any other direction. Generally, after calculating the regularity in multiple directions, the maximum regularity is taken as the judgment basis for whether the image has approximated regular texture primitives.

The INDMF regularity calculation involved in this section is encoded by MATLAB software. The version of MATLAB is 9.4 and the location is Nanjing The calculation results are saved in CSV format and used for subsequent recognition.

2.2.2. Typical Loess Landform Recognition Combined with INDMF Regularity

To test the application of the proposed INDMF regularity in the recognition of typical landforms on the Loess Plateau, the INDMF regularity is added on the basis of the existing landform recognition methods to verify whether the typical landform recognition accuracy is improved. The existing method comes from the recognition and classification method in [23,24]. The main process is as follows. The slope derivation factor and GLCM texture features for the DEM data are calculated. Then, the sample data is used to train multi-layer recognition rules. Finally, the trained rules are applied to the test data to obtain the recognition results and accuracy. The process of loess typical landform recognition combined with the structural characteristics proposed in this paper is shown in Figure 4.
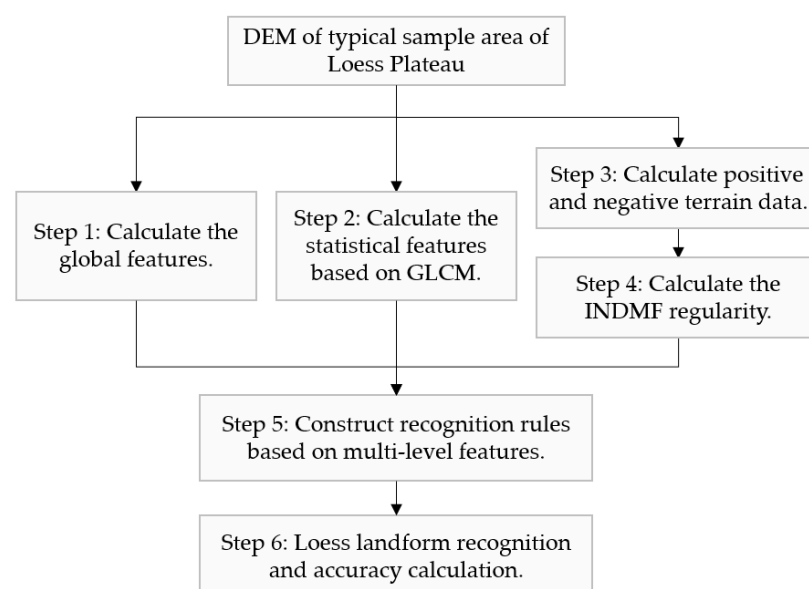
Figure 4. Flow chart of typical landform recognition of Loess Plateau combined with INDMF regularity.

As shown in Figure 4, the proposed method mainly makes two improvements on the basis of the existing methods. The first improvement is that in Steps 3 and 4, the positive and negative terrains of the DEM are calculated, effectively simplifying the DEM data, but

retaining the core valley terrain features. The second improvement is the incorporation of the INDMF regularity into the hierarchical recognition as a structural feature.

The positive and negative terrains are calculated because the morphological characteristics of the combination of the positive and negative terrains are the most intuitive and an external expression of the difference law of the loess geomorphic zone, and it is an effective carrier to express the terrain texture of the loess geomorphology [52]. Taking the loess shoulder line as the boundary, the area above the line is the positive terrain, and the area below the line is the negative terrain. Through the calculation flow [53], the positive terrain is assigned as 1 and the negative terrain is assigned as 0, so as to simplify the terrain. The positive and negative terrain extraction method used in this paper is the classical neighbourhood analysis method [53] which has the following main steps: (1) set the size of the analysis window; (2) perform neighbourhood analysis based on DEM data; (3) subtract the original DEM from the neighbourhood analysis results (the grid greater than 0 is the positive terrain, and that less than 0 is the negative terrain). After obtaining the positive and negative terrain data, the INDMF regularity is calculated.

As shown in Table 2, the third level feature is added to the multi-level feature recognition rules on the basis of the existing methods [23,24]. This paper does not use all terrain data and all GLCM features but optimizes and refines them on the basis of existing research. The purpose of this is to clarify the improvement of the actual recognition effect brought by the INDMF regularity. In the first level (level 1), significant slope differences exist among the loess plain, hilly and gully, and tableland areas. The use of basic terrain factors is the most effective method. In the second level (level 2), the GLCM features based on DEM data can effectively represent the local morphological characteristics of the terrain under different quantitative parameters. GLCM contrast and homogeneity are considered to be the two most effective quantitative factors for the typical landforms of the Loess Plateau [23,24]. In the third level (level 3), using the DEM and positive and negative terrain data, the INDMF regularity is calculated to characterise the local structural characteristics of the terrain that can distinguish and quantify the structural morphological characteristics of the loess hilly and gully areas.

Table 2. Three-level recognition rules of typical landforms in the Loess Plateau.

Level	Feature Description	Feature Space Selection	Quantitative Index
level 1	global features	basic terrain factors	average slope
level 2	local morphological feature	DEM	GLCM contrast GLCM homogeneity
level 3	local structural features	DEM, positive and negative terrain data	INDMF regularity

The software used in the typical loss landform recognition method involved in this section is Weka, and its version is 3.7.8. In addition, the average slope and GLCM features involved in this section are extracted using QGIS whose version is 3.22. The calculation results are saved in CSV format.

3. Results

On the basis of the sample data of the Loess Plateau (see Section 2.1 for details), the recognition results of typical landforms of the Loess Plateau are obtained by using the INDMF regularity (see Section 2.2.1 for details) and multi-level feature recognition (see Section 2.2.2 for details).

Combined with the existing methods, using the decision tree analysis module in Weka software, the multi-level recognition rules are obtained. The flow chart of three-level recognition rules of typical landforms in the Loess Plateau is shown in Figure 5. In Level 1, the average slope (AS) can be used to effectively distinguish the plain, hilly and gully, tableland and residual tableland areas of the Loess Plateau. When the average slope of the sample area is less than 8°, the area usually has a flat terrain, and the corresponding type is

loess plain. When the average slope of the sample area exceeds 19°, the areas correspond to the hilly and mountainous areas of the Loess Plateau, including the loess hill, loess ridge, loess long ridge residual tableland and loess mountain areas. When the average slope ranges from 8° to 19°, the recognition objects corresponding to the training data in this work are loess residual tableland and loess tableland.
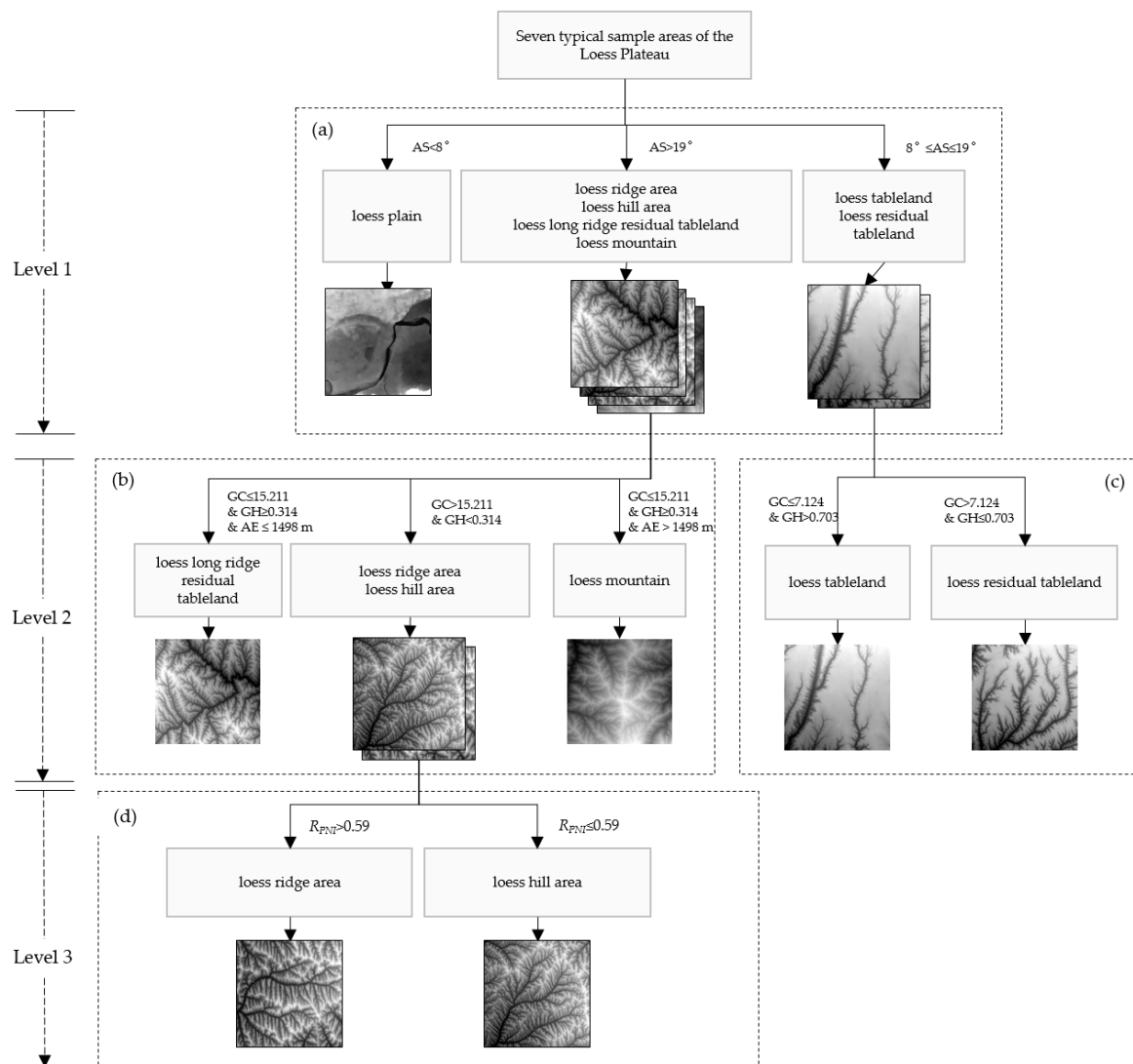
Figure 5. The flow chart of three-level recognition rules. (**a**) the first level recognition rule; (**b**) the second level recognition rule for loess gully and hilly areas; (**c**) the second level recognition rule for loess tableland; (**d**) the third level recognition rule.

The second level recognition rules (Level 2) for loess hilly areas are shown in Figure 5b,c. In Level 2, as shown in Figure 5b, the GLCM features based on the DEM data can effectively represent the local morphological characteristics of the terrain based on different quantitative parameters. According to the analysis conclusions of the existing methods and decision tree analysis module in Weka, the two most effective parameters are selected; the GLCM contrast (GC) and the GLCM homogeneity (GH). When GC is greater than 15.211 and GH is less than 0.314, it can effectively distinguish loess gully areas from loess mountain and loess long ridge residual tableland areas. For the loess mountain and long ridge residual tableland areas, a significant difference feature is DEM average elevation (AE). The AE of the loess mountain is relatively high, effectively distinguishing mountain and long ridge residual tableland areas. When GC $\leq$ 15.211 and GH $\geq$ 0.314 and the average elevation

exceeds 1498 m, the category is loess mountain areas. When GC ≤ 15.211 and GH ≥ 0.314 and the average elevation is less than or equal to 1498 m, the category is long ridge residual tableland areas.

In Level 2, the second level recognition rules for loess tableland and residual tableland areas are shown in Figure 5c. After the basic terrain factor average slope of the first level is used to distinguish these areas, the two must be subdivided. The main difference between the loess tableland and residual tableland areas lies in their different degrees of geomorphic development. The difference in surface morphology between the two can be distinguished by GLCM contrast and GLCM homogeneity. When GC ≤ 7.124 and GH > 0.703, this type is loess tableland. Conversely, when GC > 7.124 and GH ≤ 0.703, this type is loess residual tableland.

In Level 3, the DEM is used to generate positive and negative terrain data, and the INDMF regularity is calculated to characterise the local structure characteristics of the terrain. The loess top surface of the loess ridge area is well preserved and belongs to the inter gully land type. The surface erosion and rill and gully erosion on the beam slope are in the stage of accelerated development. The texture features have a regular rectangular distribution, and the width of the beam is relatively consistent. The third level recognition rules of the loess hilly and gully area are shown in Figure 5d. The positive and negative terrain INDMF regularity (R_{PNI}) is calculated as the recognition quantitative index. When $R_{PNI} > 0.59$, the area is determined as a loess ridge area. When $R_{PNI} ≤ 0.59$, the area is determined as a loess hill area.

To further test the effectiveness of the multi-level recognition rules in this paper, each sample area uses 15 samples to build a test database. In addition, another 33 confusion sample areas are added, mainly transition areas or areas with atypical geomorphic types. Test and mixed samples together add up to 138 sample areas.

In this paper, retrieval precision is used as the accuracy evaluation, rather than directly using the confusion matrix as the evaluation basis. The decision tree level is constructed according to the prior knowledge, and then the local optimal classification is carried out on the basis of the decision tree category. In the test, the retrieval precision is shown in Formula (4):

$$CP = \frac{N_C}{N_{layer\_total}} \times 100\% \tag{4}$$

where CP represents the precision of the correct category, N_C represents the number of correct categories retrieved, N_{layer_total} indicates the number of all correct categories contained in the corresponding recognition hierarchy.

According to the three-level recognition rules shown in Figure 5, the statistical table of the first level precision rate is shown in Table 3. The average slope is used for the first level classification of seven typical sample areas of the Loess Plateau. The correct precision rate for plain areas is 86.67%, that for hilly and gully and mountainous areas is 96.67%, and that for tableland and residual tableland is 93.33%. Through the average slope, three types of shapes and areas with slope differences can be significantly distinguished.

Table 3. Statistical table of the first level precision rate.

Level	Type	Correct Category Number	Sample Number	CP
	loess plain	13	15	86.67%
level 1	loess hilly and gully and mountain area	58	60	96.67%
	loess tableland area	28	30	93.33%

After the Level 1 recognition, Table 4 shows the statistical results of the second level precision rate of hilly and gully and mountain areas. According to characteristics of the GLCM contrast and GLCM homogeneity, the vector is constructed based on 64 grey levels

and combined with four directions (i.e., 0°, 45°, 90°, 135°). The feature vector can well distinguish loess long ridge residual tableland, loess hill, loess ridge and loess mountain areas. Among them, combined with the average elevation topographic data, the precision of the loess mountain area is 100%. The average elevation combined with texture features can significantly distinguish the loess mountains.

Table 4. Statistical results of the second level precision rate of hilly and gully and mountain areas.

Level	Type	Correct Category Number	Sample Number	CP
level 2	loess ridge residual tableland	12	14	85.71%
	loess hill and loess ridge area	27	30	90.00%
	loess mountain area	14	14	100.00%

Table 5 is the statistical table of the second level precision rate of loess tableland and loess residual tableland. Among them, the accurate number of loess residual tableland is 10, and the retrieval accuracy rate is 76.92%. The main difference between loess tableland and loess residual tableland lies in their different degrees of geomorphic development which shows that the degree of erosion is more intense than that of loess tableland. However, when a specific part of the Loess residual tableland is extremely broken, it will be confused with loess long ridge areas, resulting in misrecognition.

Table 5. Statistical results of the second level precision rate of tableland and residual tableland area.

Level	Type	Correct Category Number	Sample Number	CP
level 2	loess residual tableland	10	13	76.92%
	loess tableland	14	15	93.33%

Table 6 shows the statistics of the precision rate of the loess hill and loess ridge areas on the basis of the third level rule. The erosion of the loess hill area is worse than that of the loess ridge area, and the texture features are characterised by vertical and horizontal gullies in the entire area. In the loess ridge area, the texture features have a regular rectangular distribution, and the width of the loess beam is relatively consistent, with a precision rate of 92.86%. However, for the loess hill area, the regularity of some hilly hills is low, causing misclassification with the confused samples, such as loess residual tableland and loess stream land, resulting in misclassification phenomena in the hilly area, with a precision rate of 84.62%.

Table 6. Statistical results of the third level precision rate of the loess hill and loess ridge areas.

Level	Type	Correct Category Number	Sample Number	CP
level 3	loess hill area	11	13	84.62%
	loess ridge area	13	14	92.86%

4. Discussion

4.1. Effectiveness of INDMF Regularity

To test the effectiveness of the INDMF regularity, this section uses the DEM data of loess hilly and gully areas (i.e., the loess hill and loess ridge areas) for comparative analysis. From the natural surface of the Loess Plateau to the DEM and then to the positive and negative terrains, the positive terrain can be approximately expressed as significant geomorphic units, such as loess tableland, loess ridge and loess hill. Thus, in a certain area, a texture distribution mode of "macro regular and local irregular" is formed based on the positive and negative terrains to characterise the terrain texture of the Loess Plateau.

First, the loess hill area is discussed. Figure 6 contains three sample areas of the loess hill areas and the INDMF diagram of the maximum regularity direction. Taking Sample area 1 of the loess hill area as an example, as shown in Figure 6a, it is the visual effect diagram of the DEM. Figure 6b shows the positive and negative terrains extracted by the method proposed in [52], and Figure 6c is the INDMF and the red circles represent significant peaks. The image sequence of sample areas 2 and 3 in the loess hill area is consistent with that of sample area 1. Through calculation, the results of the INDMF main period and regularity in the loess hilly area are shown in Table 7.
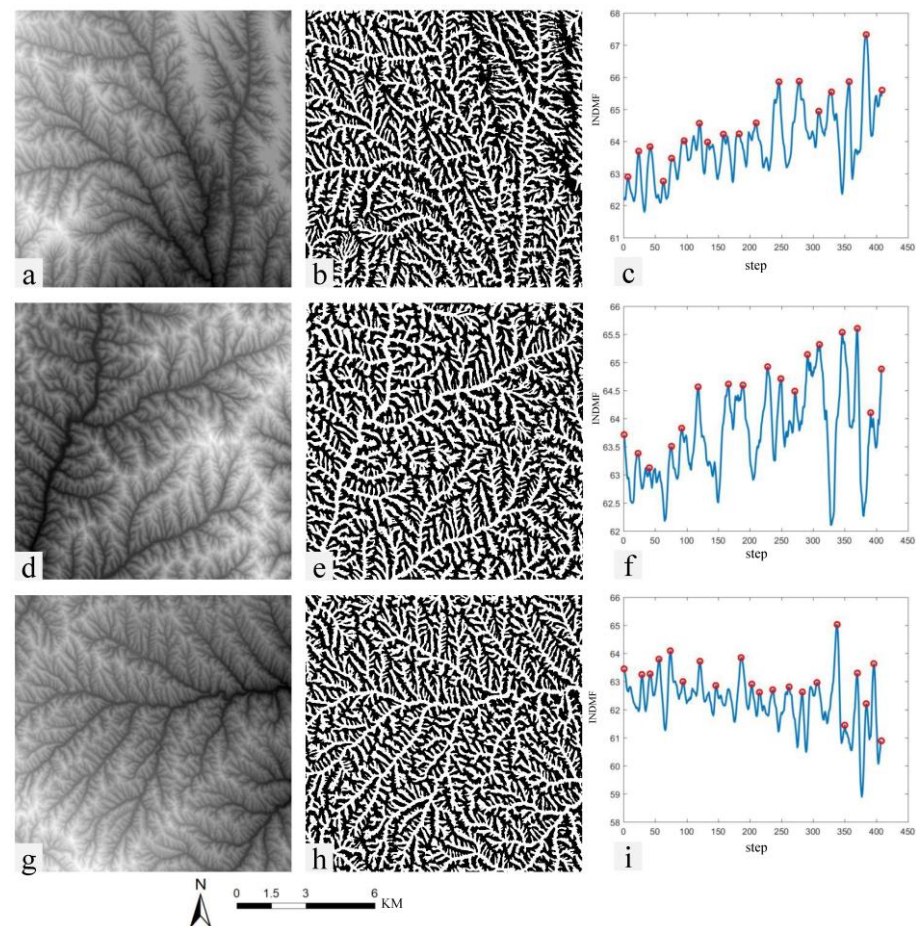
Figure 6. INDMF regularity based on loess hill areas. (**a**) sample 1; (**b**) positive and negative terrains of sample 1; (**c**) INDMF of sample 1; (**d**) sample 2; (**e**) positive and negative terrains of sample 2; (**f**) INDMF of sample 2; (**g**) sample 3; (**h**) positive and negative terrains of sample 3; (**i**) INDMF of sample 3.

Table 7. Results of main period and INDMF regularity in the loess hill areas.

Sample	Maximum Direction of Regularity	Main Period (Pixel)	INDMF Regularity
sample 1 (Figure 6a)	row direction	21	0.54
sample 2 (Figure 6d)	row direction	22	0.42
sample 3 (Figure 6g)	column direction	22	0.47
average		21.6	0.48

Then the loess ridge area is discussed. Figure 7 includes three sample areas of the loess ridge areas and the INDMF diagram in the maximum regularity direction. Taking Sample area 1 of the loess ridge area as an example, Figure 7c shows the row direction INDMF. The

image sequence of sample areas 2 and 3 is consistent with that of sample area 1, which are Figure 7d,g, respectively. The results of the INDMF main period and regularity in the loess ridge area are shown in Table 8.
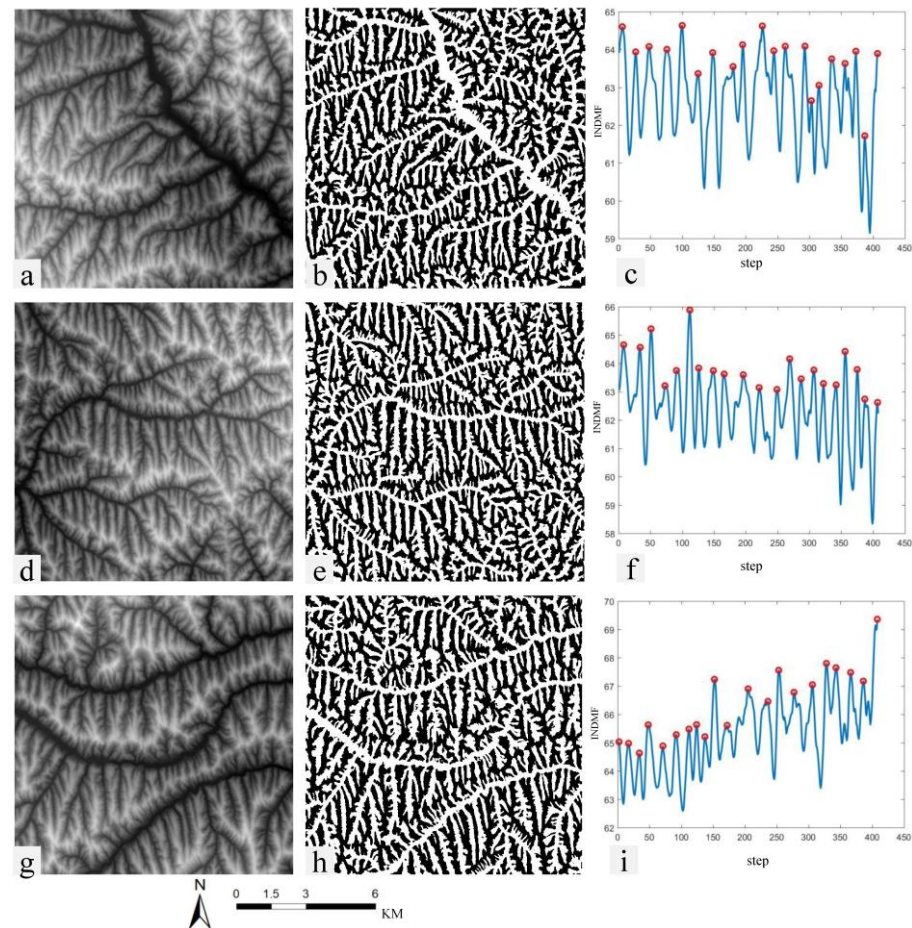

Figure 7. INDMF regularity based on loess ridge areas. (**a**) sample 1; (**b**) positive and negative terrains of sample 1; (**c**) INDMF of sample 1; (**d**) sample 2; (**e**) positive and negative terrains of sample 2; (**f**) INDMF of sample 2; (**g**) sample 3; (**h**) positive and negative terrains of sample 3; (**i**) INDMF of sample 3.

Table 8. Results of main period and INDMF regularity in the loess ridge areas.

Sample	Maximum Direction of Regularity	Main Period (Pixel)	INDMF Regularity
sample 1 (Figure 7a)	row direction	21	0.58
sample 2 (Figure 7d)	row direction	20	0.65
sample 3 (Figure 7g)	row direction	20	0.70
average		20.3	0.64

The analysis results in Figures 6 and 7 and Tables 7 and 8 indicate that the average main period of the loess hill area is 21.6 pixels, the actual distance is 540 m, and the average regularity is 0.48. The average main period of the loess ridge area is 20.3 pixels, which is basically consistent with the loess hill area. The actual distance is 507.5 m, and the average regularity is 0.64. The texture primitives of the positive and negative terrains formed by the loess ridge area have higher regularity than those formed by the loess hill area, which is consistent with the actual situation. This phenomenon occurs because the individual hills in the loess hill area are more regular than those in the loess ridge area. However, overall,

the regularity of the arrangement of the hill elements of loess hill is not as good as the beam elements of loess ridge in a certain direction, and the difference in regularity is 0.16. The above analysis indicates that facing the hilly and gully area of the Loess Plateau, the hilly and gully region can be effectively distinguished in the spatial structure arrangement on the basis of the INDMF regularity of the positive and negative terrains. INDMF regularity can provide support for the accurate recognition and classification of the loess landform. The purpose of the INDMF proposed in this paper is to obtain the approximate regularity of complex texture primitives. Due to the particularity of the loess hill and loess ridge, it is very similar to primitives in texture images. Therefore, the INDMF method is used in this paper. The INDMF method can approximately quantify the shape and spatial distance of the principal texture primitives of loess hill and loess ridge, which can be used as one of the important quantitative indexes.

4.2. Role of Positive and Negative Terrain in Recognition

The geomorphic form of thousands of gullies on the Loess Plateau shows the most external and core geomorphic features between gullies through the staggered distribution of the positive and negative topography and the twists and turns along the gullies [53–55]. Zhou et al. [53] summarised the characteristics of positive and negative terrains as follows: the first characteristic is macro abstraction. The positive and negative topographies of the Loess Plateau are the most dominant binary structure model in the Loess geomorphic system. The combined form of the positive and negative topographies is the abstraction and generalisation of the macro form of the loess geomorphology. The second characteristic is quantifiability. Quantitative analysis can be carried out through the attribute characteristics of the positive and negative terrains, such as area, elevation mean value and slope characteristics of DEM, or through the relationship between the positive and negative terrains, such as correlation degree, spatial distribution and other characteristics. The third characteristic is geomorphic correspondence. Different geomorphic types of Loess Plateau correspond to different forms of positive and negative topographies. According to the quantifiable characteristics of morphology, different geomorphic types of loess can be analysed quantitatively.

For real-world terrain data, there are often interference factors, so INDMF usually needs to be used together with a terrain simplification algorithm to achieve better results. This paper uses positive and negative terrain, which is essentially a way of terrain simplification. Taking the loess shoulder line as the boundary, the area above the line is the positive terrain, and the area below the line is the negative terrain. Through the calculation flow [53], the positive terrain is assigned as 1 and the negative terrain is assigned as 0, so as to simplify the terrain. In the hilly and gully region of the Loess Plateau, for the regions with significant positive and negative terrains, Figure 8a shows the loess hilly and gully region, such as the Suide and Lishi. Figure 8b shows the loess tableland area, such as the Luochuan. For the positive and negative terrains shown in Figure 8a, the positive terrain includes beam and ridge top and gully slope, and the negative terrain is loess gully. For the positive and negative terrains shown in Figure 8b, the positive terrain mainly includes tableland surface and ridge slope, and the negative terrain is also loess gully [21,56]. The topographic texture of the Loess Plateau is the spatial distribution pattern formed by the arrangement and combination of loess geomorphic units. Among them, the geomorphic unit is the texture primitive. Through the definition and the characteristics of the positive and negative terrains, the positive and negative terrain unit can be simplified and abstracted into the texture primitive of the terrain texture of the Loess Plateau. From the natural surface of the Loess Plateau to the DEM and then to the positive and negative terrains, the positive terrain can be approximately expressed as significant geomorphic units, such as tableland, beam, hill, sand dune and gully. Thus, in a certain area, a texture distribution mode of "macro regular and local irregular" is formed based on the positive and negative terrains to characterise the terrain texture of the Loess Plateau.
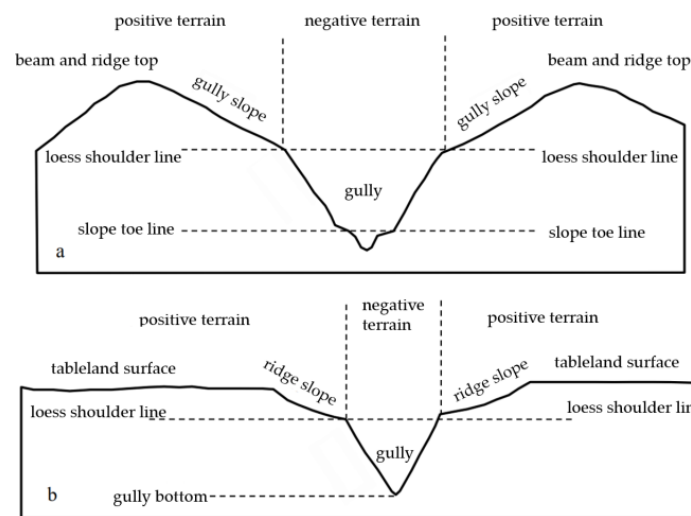
Figure 8. Schematic of the positive and negative topography of the Loess Plateau [55]. (**a**) loess hilly and gully area; (**b**) loess tableland area.

When positive terrain and negative terrain are not used, due to the interference of a large number of secondary texture primitives on DEM, the regularity of the loess ridge area and loess hill area is close to 0, that is, both of them show an irregular phenomenon. Section 4.1 shows that the positive and negative terrains can indeed reduce the noise interference in the DEM data of the real terrain and retain the characteristics of the most core ditches and valleys in the Loess Hills, providing a data basis for effectively extracting the regularity.

4.3. Scope of Application of the Regularity Proposed in This Paper

The two innovations of this paper are: (1) taking INDMF as the basic model, this paper constructs a terrain regularity calculation method based on DEM data. This method can effectively reduce various interference factors in the terrain and extract the regularity of main terrain units. (2) The regularity is applied to the classification of loess landforms, so as to improve the recognition accuracy of hilly and gully areas of the Loess Plateau. Then, for the regularity in contribution 1 of this paper, can we apply it to the recognition of other landforms? Can it be used elsewhere? The key to its applicability is whether the landform unit (or texture primitive) has structural characteristics in spatial distribution. According to this judgment condition and the author's follow-up research, at least two cases can use the regularity of this paper as one of the characteristics: the first is the artificial landform, and the second is the natural landform with significant structural characteristics.

For artificial landforms, Yalniz and Aksoy [42] have applied regularity calculation to the identification of artificial vegetation. Another important artificial landform is terraced fields, including terraced fields on the Loess Plateau [10,57] and Honghe Hani rice terraces [58]. Terraced fields show obvious stripe texture on DEM data, which is suitable for the operation of regularity. Taking the terraced fields on the Loess Plateau as an example, Figure 9 shows the DEM-based hillshade map of a small watershed on the Loess Plateau of China. Figure 9a corresponds to the terraced field, and Figure 9b corresponds to the gully bottom area with serious erosion. Through the authors' regularity calculation, it is found that the regularity of Figure 9a is significantly higher than that of Figure 9b. At the same time, it is found that the regularity between different terraced fields also has numerical differences. Therefore, regularity can become one of the important indicators to identify terraced fields. In addition to artificial landforms, natural landforms with significant structural characteristics can also use the regularity proposed in this paper. One of the cases is Telbisz and Keszler's [59] research on DEM-based sand dune patterns. The other case is from Ely, et al. [60] for the research on Drumlins. The above two research objects have significant structural texture features and have the potential to use the regularity of this

paper. In addition, the terrain of the hilly and gully region of the Iranian Loess Plateau is similar to that of the Chinese Loess Plateau [61], which also provides the possibility for the subsequent use of regularity. Moreover, with the development of deep learning in landform classification [62,63], the regularity proposed may also become one of its effective features.
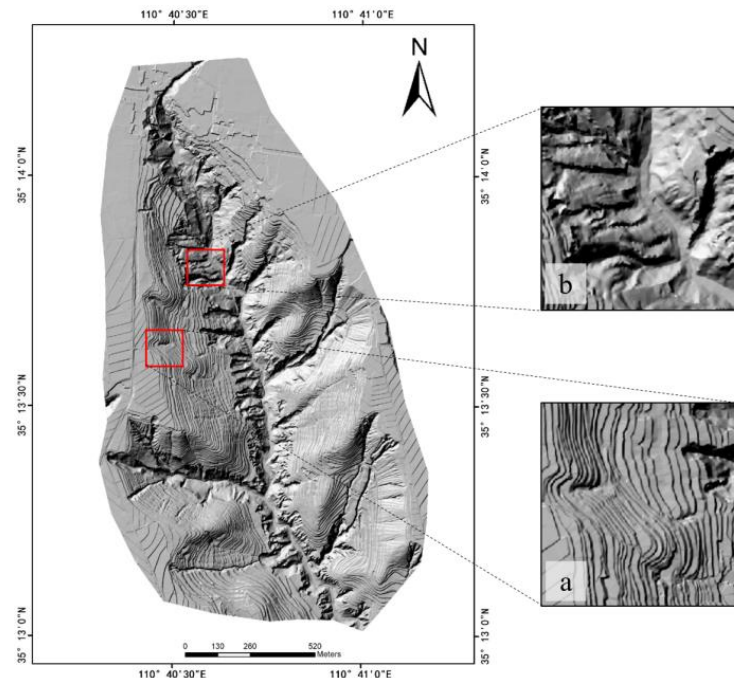
Figure 9. DEM based hillshade map of a small watershed in the Loess Plateau of China. (**a**) terraced field; (**b**) gully bottom area.

5. Conclusions

Taking the Loess Plateau as the study area and the 25 m/pixel DEM as the sample data, a regularity calculation method based on the INDMF is proposed and applied to the recognition experiment on typical landforms on the Loess Plateau. The results of the experiment show that the average regularity of the loess hill area is 0.48 and that of the loess ridge area is 0.64. Based on this, the INDMF regularity can effectively distinguish loess hill areas and loess ridge areas. To further test the application of the structural characteristics of regularity in the recognition of typical landforms on the Loess Plateau, this paper adds INDMF regularity on the basis of the existing landform recognition methods. The recognition rules based on multi-level features are applied to the test data. The experimental results show that compared with previous methods, adding structural features (i.e., INDMF regularity) can effectively distinguish loess hills and loess ridges in the hilly and gully regions. For loess hills and loess ridges, the recognition rates of the proposed method are 84.62% and 92.86%, respectively. Combined with the existing topographic characteristics, the proposed INDMF regularity is a topographic structure feature extraction method that can effectively discriminate between loess hill and loess ridge areas on the Loess Plateau.

The purpose of the INDMF proposed in this paper is to obtain the approximate regularity of complex texture primitives. Due to the particularity of the loess hill and loess ridge landform, it is very similar to the primitive texture image, so it is suitable for the INDMF method used in this paper. The INDMF method can quantify the shape and spatial distance of the principal texture primitives of loess hill and loess ridge, which can be used as one of the important quantitative indexes. For other loess areas of the world, if the region has significant spatial distribution characteristics of texture primitives, INDMF regularity can also be used to extract regularity and quantify features. At the same time, we also see that the use of INDMF features has limitations. For real terrain data, it often has a lot of noise. Therefore, INDMF usually needs to be used together with a terrain simplification

algorithm to achieve good results. This paper uses positive and negative terrain for terrain simplification.

References

1. Yang, S.; Ding, Z. Comparison of particle size characteristics of the Tertiary 'red clay'and Pleistocene loess in the Chinese Loess Plateau: Implications for origin and sources of the 'red clay'. *Sedimentology* **2004**, *51*, 77–93. [CrossRef]
2. Maher, B.A. Palaeoclimatic records of the loess/palaeosol sequences of the Chinese Loess Plateau. *Quat. Sci. Rev.* **2016**, *154*, 23–84. [CrossRef]
3. Fenn, K.; Stevens, T.; Bird, A.; Limonta, M.; Rittner, M.; Vermeesch, P.; Andò, S.; Garzanti, E.; Lu, H.; Zhang, H. Insights into the provenance of the Chinese Loess Plateau from joint zircon U-Pb and garnet geochemical analysis of last glacial loess. *Quat. Res.* **2018**, *89*, 645–659. [CrossRef]
4. Wen, X.; Zhen, L. Soil erosion control practices in the Chinese Loess Plateau: A systematic review. *Environ. Dev.* **2020**, *34*, 100493. [CrossRef]
5. Wei, H.; Li, S.; Li, C.; Zhao, F.; Xiong, L.; Tang, G. Quantification of Loess Landforms from Three-Dimensional Landscape Pattern Perspective by Using DEMs. *ISPRS Int. J. Geo-Inf.* **2021**, *10*, 693. [CrossRef]
6. Yang, H.; Liu, J.; Bai, L.; Luo, M. Similarity Analysis: Revealing the Regional Difference in Geomorphic Development in Areas with High and Coarse Sediment Yield of the Loess Plateau in China. *ISPRS Int. J. Geo-Inf.* **2022**, *11*, 227. [CrossRef]
7. Song, Y.; Xue, D.; Dai, L.; Wang, P.; Huang, X.; Xia, S. Land cover change and eco-environmental quality response of different geomorphic units on the Chinese Loess Plateau. *J. Arid Land* **2020**, *12*, 29–43. [CrossRef]
8. Hu, S.; Qiu, H.; Wang, N.; Cui, Y.; Wang, J.; Wang, X.; Ma, S.; Yang, D.; Cao, M. The influence of loess cave development upon landslides and geomorphologic evolution: A case study from the northwest Loess Plateau, China. *Geomorphology* **2020**, *359*, 107167. [CrossRef]
9. Ding, H.; Liu, K.; Chen, X.; Xiong, L.; Tang, G.; Qiu, F.; Strobl, J. Optimized segmentation based on the weighted aggregation method for loess bank gully mapping. *Remote Sens.* **2020**, *12*, 793. [CrossRef]
10. Ding, H.; Na, J.; Jiang, S.; Zhu, J.; Liu, K.; Fu, Y.; Li, F. Evaluation of Three Different Machine Learning Methods for Object-Based Artificial Terrace Mapping—A Case Study of the Loess Plateau, China. *Remote Sens.* **2021**, *13*, 1021. [CrossRef]
11. Jiang, C.; Fan, W.; Yu, N.; Nan, Y. A New Method to Predict Gully Head Erosion in the Loess Plateau of China Based on SBAS-InSAR. *Remote Sens.* **2021**, *13*, 421. [CrossRef]
12. Liu, Z.; Liu, Y. Does anthropogenic land use change play a role in changes of precipitation frequency and intensity over the Loess Plateau of China? *Remote Sens.* **2018**, *10*, 1818. [CrossRef]
13. Na, J.; Yang, X.; Tang, G.; Dang, W.; Strobl, J. Population characteristics of loess gully system in the Loess Plateau of China. *Remote Sens.* **2020**, *12*, 2639. [CrossRef]
14. Tao, Y.; Wang, C.; Jiang, S. A new method on terrain texture characteristics extraction based on improved dual-tree complex wavelet transform. *Geogr. Geo-Inf. Sci.* **2017**, *33*, 47–50.
15. Na, J.; Ding, H.; Zhao, W.; Liu, K.; Tang, G.; Pfeifer, N. Object-based large-scale terrain classification combined with segmentation optimization and terrain features: A case study in China. *Trans. GIS* **2021**, *25*, 2939–2962. [CrossRef]
16. Xiong, L.; Tang, G.; Li, F.; Yuan, B.; Lu, Z. Modeling the evolution of loess-covered landforms in the Loess Plateau of China using a DEM of underground bedrock surface. *Geomorphology* **2014**, *209*, 18–26. [CrossRef]
17. Zhao, G.; Mu, X.; Wen, Z.; Wang, F.; Gao, P. Soil erosion, conservation, and eco-environment changes in the Loess Plateau of China. *Land Degrad. Dev.* **2013**, *24*, 499–510. [CrossRef]
18. Jin, F.; Yang, W.; Fu, J.; Li, Z. Effects of vegetation and climate on the changes of soil erosion in the Loess Plateau of China. *Sci. Total Environ.* **2021**, *773*, 145514. [CrossRef]

19. Li, P.; Wang, J.; Liu, M.; Xue, Z.; Bagherzadeh, A.; Liu, M. Spatio-temporal variation characteristics of NDVI and its response to climate on the Loess Plateau from 1985 to 2015. *Catena* **2021**, *203*, 105331. [CrossRef]
20. Tang, G.; Na, J.; Cheng, W. Progress of digital terrain analysis on regional geomorphology in China. *Acta Geod. Cartogr. Sin.* **2017**, *46*, 1570.
21. Xiong, L.; Tang, G.; Yang, X.; Li, F. Geomorphology-oriented digital terrain analysis: Progress and perspectives. *J. Geogr. Sci.* **2021**, *31*, 456–476. [CrossRef]
22. Tao, Y. Texture Analysis Based Research on Terrain Morphology Characteristics. Ph.D. Thesis, Nanjing Normal University, Nanjing, China, 2013.
23. Liu, K.; Tang, G.A.; Huang, X. Research on the difference between textures derived from DEM and remotesensing image for topographic analysis. *J. Geoinf. Sci.* **2016**, *18*, 386–395.
24. Huang, X.; Liu, K. The Influence of DEM resolution on the extraction of terrain texture feature. *J. Geo-Inf. Sci.* **2015**, *17*, 822–829.
25. Li, K.; Yan, S. Scale Stability investigation based on RILBP for terrain structure. *Geogr. Geo-Inf. Sci.* **2017**, *33*, 63–68.
26. Ding, H.; Na, J.-M.; Huang, X.-L.; Tang, G.-A.; Liu, K. Stability analysis unit and spatial distribution pattern of the terrain texture in the northern Shaanxi Loess Plateau. *J. Mt. Sci.* **2018**, *15*, 577–589. [CrossRef]
27. Zhao, G.; Kondolf, G.M.; Mu, X.; Han, M.; He, Z.; Rubin, Z.; Wang, F.; Gao, P.; Sun, W. Sediment yield reduction associated with land use changes and check dams in a catchment of the Loess Plateau, China. *Catena* **2017**, *148*, 126–137. [CrossRef]
28. Li, X.; Yang, H.; Yin, Z. Regional loess landslide recognition method research based on DEM and remote sensing image. *Geogr. Geo-Inf. Sci.* **2017**, *33*, 86–92.
29. Xu, Y.; Zhu, H.; Hu, C.; Liu, H.; Cheng, Y. Deep learning of DEM image texture for landform classification in the Shandong area, China. *Front. Earth Sci.* **2021**, 1–16. [CrossRef]
30. Wu, Q.; Song, C.; Liu, K.; Ke, L. Integration of TanDEM-X and SRTM DEMs and spectral imagery to improve the large-scale detection of opencast mining areas. *Remote Sens.* **2020**, *12*, 1451. [CrossRef]
31. Blaschke, T.; Feizizadeh, B.; Hölbling, D. Object-based image analysis and digital terrain analysis for locating landslides in the Urmia Lake Basin, Iran. *IEEE J. Sel. Top. Appl. Earth Obs. Remote Sens.* **2014**, *7*, 4806–4817. [CrossRef]
32. Liu, K.; Ding, H.; Tang, G.; Zhu, A.-X.; Yang, X.; Jiang, S.; Cao, J. An object-based approach for two-level gully feature mapping using high-resolution DEM and imagery: A case study on hilly loess plateau region, China. *Chin. Geogr. Sci.* **2017**, *27*, 415–430. [CrossRef]
33. Haralick, R.M. Statistical and structural approaches to texture. *Proc. IEEE* **1979**, *67*, 786–804. [CrossRef]
34. Franklin, S.E.; Peddle, D.R. Texture analysis of digital image data using spatial cooccurrence. *Comput. Geosci.* **1987**, *13*, 293–311. [CrossRef]
35. Tang, G.; Li, F.; Xiong, L. Progress of digital terrain analysis in the Loess Plateau of China. *Geogr. Geo-Inf. Sci.* **2017**, *33*, 1–7.
36. Tang, G. Progress of DEM and digital terrain analysis in China. *Acta Geogr. Sin.* **2014**, *69*, 1305–1325.
37. Leu, J.-G. On indexing the periodicity of image textures. *Image Vis. Comput.* **2001**, *19*, 987–1000. [CrossRef]
38. Lin, H.-C.; Wang, L.-L.; Yang, S.-N. Regular-texture image retrieval based on texture-primitive extraction. *Image Vis. Comput.* **1999**, *17*, 51–63. [CrossRef]
39. Chetverikov, D.; Hanbury, A. Finding defects in texture using regularity and local orientation. *Pattern Recognit.* **2002**, *35*, 2165–2180. [CrossRef]
40. Matsuyama, T.; Miura, S.-I.; Nagao, M. Structural analysis of natural textures by Fourier transformation. *Comput. Vis. Graph. Image Process.* **1983**, *24*, 347–362. [CrossRef]
41. Escofet, J.; Millán, M.S.; Ralló, M. Modeling of woven fabric structures based on Fourier image analysis. *Appl. Opt.* **2001**, *40*, 6170–6176. [CrossRef]
42. Yalniz, I.Z.; Aksoy, S. Unsupervised detection and localization of structural textures using projection profiles. *Pattern Recognit.* **2010**, *43*, 3324–3337. [CrossRef]
43. Conners, R.W.; Harlow, C.A. Toward a structural textural analyzer based on statistical methods. *Comput. Graph. Image Process.* **1980**, *12*, 224–256. [CrossRef]
44. Oh, G.; Lee, S.; Shin, S.Y. Fast determination of textural periodicity using distance matching function. *Pattern Recognit. Lett.* **1999**, *20*, 191–197. [CrossRef]
45. Asha, V.; Nagabhushan, P.; Bhajantri, N.U. Automatic extraction of texture-periodicity using superposition of distance matching functions and their forward differences. *Pattern Recognit. Lett.* **2012**, *33*, 629–640. [CrossRef]
46. Chetverikov, D. Pattern regularity as a visual key. *Image Vis. Comput.* **2000**, *18*, 975–985. [CrossRef]
47. Morales, R.L.; Yanez, R.E.S.; Ramírez, V.A. Periodicity and texel size estimation of visual texture using entropy cues. *Comput. Sist.* **2011**, *14*, 303–319.
48. Jiang, S.; Tang, G.; Liu, K. A computation method of texture regularity using summed-up distance matching function. *J. Comput. -Aided Des. Comput. Graph.* **2015**, *27*, 1874–1880.
49. Jiang, S.; Tang, G.; Tao, Y. Automatic Extraction Method for Texture Periodicity Based on Improved Normalized Distance Matching Function. *Pattern Recognit. Artif. Intell.* **2014**, *27*, 1098–1104.
50. Yuan, B.; Tang, G.; Zhou, L.; Hao, Q.; Li, F.; Lu, Z. Control action on the geomorphic differentiation in Loess Plateau and the formation of Yellow River by Cenozoic tectogenesis. *Quat. Sci.* **2012**, *32*, 829–838.

51. Liu, K.; Tang, G.; Tao, Y.; Jiang, S. GLCM based quantitative analysis of terrain texture from DEMs. *J. Geo-Inf. Sci.* **2012**, *14*, 751–760. [CrossRef]

52. Zhou, C.; Cheng, W.; Qian, J.; Li, B.; Zhang, B. Research on the classification system of digital land geomorphology of 1:10,00,000 in China. *J. Geo-Inf. Sci.* **2009**, *11*, 707–724.

53. Zhou, Y.; Tang, G.; Yang, X.; Xiao, C.; Zhang, Y.; Luo, M. Positive and negative terrains on northern Shaanxi Loess Plateau. *J. Geogr. Sci.* **2010**, *20*, 64–76. [CrossRef]

54. Yang, F.; Zhou, Y. Quantifying spatial scale of positive and negative terrains pattern at watershed-scale: Case in soil and water conservation region on Loess Plateau. *J. Mt. Sci.* **2017**, *14*, 1642–1654. [CrossRef]

55. Cao, M.; Tang, G.A.; Zhang, F.; Yang, J. A cellular automata model for simulating the evolution of positive–negative terrains in a small loess watershed. *Int. J. Geogr. Inf. Sci.* **2013**, *27*, 1349–1363. [CrossRef]

56. Xiong, L.; Tang, G.; Yan, S.; Zhu, S.; Sun, Y. Landform-oriented flow-routing algorithm for the dual-structure loess terrain based on digital elevation models. *Hydrol. Process.* **2014**, *28*, 1756–1766. [CrossRef]

57. Zhou, Q.; Xu, Q.; Peng, D.; Fan, X.; Ouyang, C.; Zhao, K.; Li, H.; Zhu, X. Quantitative spatial distribution model of site-specific loess landslides on the Heifangtai terrace, China. *Landslides* **2021**, *18*, 1163–1176. [CrossRef]

58. Wang, Z.; Marafa, L. Tourism Imaginary and Landscape at Heritage Site: A Case in Honghe Hani Rice Terraces, China. *Land* **2021**, *10*, 439. [CrossRef]

59. Telbisz, T.; Keszler, O. DEM-based morphometry of large-scale sand dune patterns in the Grand Erg Oriental (Northern Sahara Desert, Africa). *Arab. J. Geosci.* **2018**, *11*, 382. [CrossRef]

60. Ely, J.C.; Clark, C.D.; Spagnolo, M.; Hughes, A.L.; Stokes, C.R. Using the size and position of drumlins to understand how they grow, interact and evolve. *Earth Surf. Process. Landf.* **2018**, *43*, 1073–1087. [CrossRef]

61. Maleki, S.; Khormali, F.; Mohammadi, J.; Bogaert, P.; Bodaghabadi, M.B. Effect of the accuracy of topographic data on improving digital soil mapping predictions with limited soil data: An application to the Iranian loess plateau. *Catena* **2020**, *195*, 104810. [CrossRef]

62. Li, S.; Hu, G.; Cheng, X.; Xiong, L.; Tang, G.; Strobl, J. Integrating topographic knowledge into deep learning for the void-filling of digital elevation models. *Remote Sens. Environ.* **2022**, *269*, 112818. [CrossRef]

63. Li, S.; Xiong, L.; Tang, G.; Strobl, J. Deep learning-based approach for landform classification from integrated data sources of digital elevation model and imagery. *Geomorphology* **2020**, *354*, 107045. [CrossRef]